Journal of Experimental Botany, Vol. 61, No. 5, pp. 1375–1383, 2010
doi:10.1093/jxb/erq006 Advance Access publication 16 February, 2010
This paper is available online free of all access charges (see http://jxb.oxfordjournals.org/open_access.html for further details)

Journal of Experimental Botany
www.jxb.oxfordjournals.org

RESEARCH PAPER

Contribution of carbon fixed by Rubisco and PEPC to phloem export in the Crassulacean acid metabolism plant *Kalanchoë daigremontiana*

Birgit Wild[1,*], Wolfgang Wanek[1], Wolfgang Postl[2] and Andreas Richter[1]

[1] Department of Chemical Ecology and Ecosystem Research, University of Vienna, Althanstrasse 14, A-1090 Vienna, Austria
[2] Department of Molecular Systems Biology, University of Vienna, Althanstraße 14, A-1090 Vienna, Austria

* To whom correspondence should be addressed: E-mail: birgit.wild@univie.ac.at

Received 23 October 2009; Revised 23 December 2009; Accepted 4 January 2010

Abstract

Crassulacean acid metabolism (CAM) plants exhibit a complex interplay between CO_2 fixation by phosphoenolpyruvate carboxylase (PEPC) and ribulose-1,5-*bis*phosphate carboxylase oxygenase (Rubisco), and carbon demand for CAM maintenance and growth. This study investigated the flux of carbon from PEPC and direct Rubisco fixation to different leaf carbon pools and to phloem sap over the diurnal cycle. Concentrations and carbon isotope compositions of starch, soluble sugars, and organic acids were determined in leaves and phloem exudates of *Kalanchoë daigremontiana* Hamet et Perr., and related to CO_2 fixation by PEPC and Rubisco. Three types of leaf carbon pools could be distinguished. (i) Starch and malate pools were dominant and showed a pattern of reciprocal mobilization and accumulation (85/54 and 13/48 mg C g^{-1} DW, respective, at the beginning/end of phase I). The carbon isotope composition of these pools was compatible with predominant PEPC fixation ($\delta^{13}C$ values of –13 and –11‰ for starch and malate compared to –11‰ of PEPC fixed carbon). (ii) Isotopic composition (–17‰ and –14‰) and concentration of glucose and fructose (2 and 3 mg C g^{-1} DW, respectively) were not affected by diurnal metabolism, suggesting a low turnover. (iii) Sucrose (1–3 mg C g^{-1} DW), in contrast, exhibited large diurnal changes in $\delta^{13}C$ values (from –17‰ in the evening to –12‰ in the morning), which were not matched by net changes in sucrose concentration. This suggests a high sucrose turnover, fed by nocturnal starch degradation and direct Rubisco fixation during the day. A detailed dissection of the carbon fixation and mobilization pattern in *K. daigremontiana* revealed that direct fixation of Rubisco during the light accounted for 30% of phloem sucrose, but only 15% of fixed carbon, indicating that carbon from direct Rubisco fixation was preferentially used for leaf export.

Key words: Compound-specific isotope analysis, malate, PEPC, Rubisco, starch, sucrose.

Introduction

Crassulacean acid metabolism (CAM) is performed by about 6% of vascular plant species (Winter and Smith, 1996), mainly occurring in habitats that are affected by drought, such as deserts and tropical forest canopies. In CAM, CO_2 uptake occurs at night when relative humidity is high, thus reducing water loss from open stomata and enabling the plant to survive dry conditions. The diurnal cycle of CAM can be divided into four phases (Osmond, 1978): The period of night-time CO_2 fixation catalysed by phosphoenolpyruvate carboxylase (PEPC) and the accumulation of malate in the vacuole is denoted as phase I. With the onset of light, phase II follows, characterized by a decline in PEPC fixation and, eventually, a certain amount of direct C_3-like fixation by Rubisco. Phase III starts with stomatal closure in the late morning, when malate is decarboxylated and the released CO_2 is refixed by Rubisco. In the afternoon, stomata may re-open for direct CO_2 fixation by Rubisco in phase IV. The duration of the phases and amplitudes of CO_2 uptake differ widely between species and environmental conditions and, in particular,

additional direct fixation of CO_2 by Rubisco (phases II and IV) is highly variable (for a review see Dodd *et al.*, 2002).

The balance of mobilization and accumulation of storage carbohydrates, which accompanies the mobilization and accumulation of malate, is an important feature of CAM. In phase I, CO_2 is attached to the C_3 molecule phosphoenolpyruvate (PEP), derived from the breakdown of storage carbohydrates (usually starch or soluble sugars), resulting in the formation of the C_4 molecule malate. During the day, this carbohydrate pool has to be refilled for the subsequent night (Winter and Smith, 1996). CAM plants need to maintain a high pool of easily available carbohydrates for photosynthesis. A low level of carbohydrates for PEP generation may lead to a limited fixation of CO_2 by PEPC (Dodd *et al.*, 2003), which, in turn, would further reduce carbohydrate stocks. Thus, the maintenance of CAM, and, in consequence, the ability to cope with unfavourable environmental conditions, depends on the availability of these carbohydrates. This necessity to maintain large carbohydrate stocks, together with the high energy demand caused by conversions between metabolites and intracellular transport processes, is limiting the productivity of CAM plants. Nevertheless, some CAM plants exhibit growth rates close to C_3 plants (Nobel, 1991) – therefore, highly coordinated control mechanisms have to be assumed that regulate the competition between carbohydrate storage and growth.

To investigate the proportions of PEPC and direct Rubisco fixation in CAM plants, the analysis of C isotope composition (usually expressed as $\delta^{13}C$) has become a useful tool. Rubisco discriminates between ^{12}C and ^{13}C, leading to strongly depleted $\delta^{13}C$ values between –25‰ and –30‰ which are characteristic for C_3 metabolism. Discrimination, of course, is also influenced by environmental conditions in C_3 plants, mainly via limitations in CO_2 diffusion. Thus, under drier conditions, i.e. when stomatal resistance increases, discrimination is less pronounced (Farquhar *et al.*, 1989). PEPC on the other hand does not or only marginally discriminate against the heavier C isotope (Farquhar *et al.*, 1989). The discrimination during re-fixation of CO_2 from malate by Rubisco is only pronounced when CO_2 is leaking from the leaf (Griffiths *et al.*, 1990), which is usually considered to be low. Carbon originally fixed by PEPC (although re-fixed by Rubisco, assuming no leakage) therefore has $\delta^{13}C$ values between –8‰ and –10‰, which is close to the atmospheric value of about –8‰. Thus, the proportions of both pathways can be estimated by the plant $\delta^{13}C$ values (Winter and Holtum, 2002), provided that mesophyll conductance did not influence discrimination (Griffiths *et al.*, 2007) and that PEPC and direct Rubisco fixation have contributed proportionally to the biomass in the analysed tissue. Improving the resolution of this approach, Deleens and Garnier-Dardart (1977) and Deleens *et al.* (1979) separated biochemical fractions of *Kalanchoë* species performing CAM, and demonstrated differences in $\delta^{13}C$ values between different metabolites. Starch, organic acids, and phosphorylated compounds were generally ^{13}C enriched compared to soluble sugars and cellulose, giving rise to the idea of a compartmentation of C derived from PEPC and direct Rubisco fixation. Furthermore, C from direct daytime fixation of atmospheric CO_2 might be preferentially exported from the leaf compared to C from night-time fixation, both in *Kalanchoë pinnata* (Lam.) Pers. (Mayoral and Medina, 1985) and in *Clusia rosea* Jacq., which showed C_3-like isotope composition of fruits in contrast to far more PEPC-like signals in leaves (Borland and Dodd, 2002).

Thus, it was hypothesized that the delicate balance of C partitioning between carbohydrate storage for maintenance of photosynthetic capacity and growth was facilitated by the separate use of C from PEPC and direct Rubisco fixation. C from PEPC fixation was dedicated to the maintenance of CAM, whereas C from direct Rubisco fixation in phases II and IV was exported to sink organs, for example, inflorescences, roots or new shoots. Although C partitioning between CAM maintenance and export has been estimated by calculating C budgets from changes in pool sizes between dawn and dusk, refined by isotope signatures (Borland, 1996; Borland and Dodd, 2002), the isotopic composition and metabolic origin of exported C has not yet been directly measured in the exported C (i.e. in the phloem sap). With the recent improvements in compound-specific stable isotope analysis, i.e. HPLC systems that are directly coupled to isotope ratio mass spectrometers, more detailed analyses of such C fluxes became feasible.

Against this background, the present study aimed to clarify carbon partitioning in *K. daigremontiana*, a well-investigated CAM plant that utilizes starch as a storage carbohydrate and malic enzyme as the major decarboxylase (Christopher and Holtum, 1996). It is hypothesized that carbon from direct Rubisco fixation in phases II and IV is preferentially exported to sink tissues, while carbon originating from phase I is predominantly used for replenishment of the carbohydrate pool for CAM maintenance.

Towards this goal, plants were subjected to environmental conditions favouring PEPC fixation, with direct Rubisco fixation accounting for only 15% of daily CO_2 fixation. Gas exchange and instantaneous discrimination were measured over the diurnal cycle, as well as concentrations and $\delta^{13}C$ values of organic acids, soluble sugars, and starch. Phloem exudates were collected and analysed for $\delta^{13}C$, providing the first direct measurement of phloem isotopic composition in a CAM plant.

Materials and methods

Plant material

Kalanchoë daigremontiana Hamet et Perr. plants were precultivated in a greenhouse and transferred to a climate chamber 5 months before the start of the experiment. Plants were watered daily and fertilized with 0.2% Wuxal top N (Kwizda Agro GmbH, Vienna, Austria) every 3–4 weeks. The light period lasted from 07.00 h to 23.00 h, with light intensity increasing from dawn to 11.00 h, reaching an average midday intensity of 550 μmol m^{-2} s^{-1} at plant height. Starting at 19.00 h, the light intensity was gradually reduced, simulating natural conditions. Air temperature was

25/18 °C during the light and dark periods, respectively, and relative air humidity was constant at 60%.

When harvested, plants had 4–5 mature leaf pairs. Leaves were excised, weighed, and scanned to determine leaf area. One leaf of each pair was used for phloem exudation, and the other for the determination of soluble sugars, organic acids, and starch, where the leaves of each plant were pooled. For starch analysis, discs (diameter 0.8 cm) were punched out using a cork borer, weighed, and dried at 60 °C. Tissue saps for the determination of soluble sugars and organic acids were produced from the residual leaves by transferring them into 20 ml polyethylene flasks, heating them in a microwave oven for 10 s at 900 W to stop enzymatic activity (Popp *et al.*, 1996) and freezing them to destroy the cell membranes. Syringes containing discs of filter paper (Whatman GF/F Glass Microfibre Filters, Cat. No. 1825 025, Whatman International Ltd., Maidstone, UK) were placed in centrifuge vials, filled with the thawed samples, and centrifuged at 10 845 *g* for 10 min to collect tissue sap. Tissue saps were analysed for organic acids with HPLC-IRMS (see below). For sugars, tissue saps were treated with ion-exchange cartridges to remove ionic components (OnGuard II H 1cc cartridges and OnGuard II A 1cc, Dionex Corporation, Sunnyvale, CA, USA) before analysis with HPLC-IRMS.

To get phloem sap, leaves were recut with a razor blade at the base of the petiole. Each leaf was then inserted with the petiole into a vial containing 1.5 ml of 15 mM sodium hexametaphosphate (Fluka, Sigma-Aldrich, St Louis, MO, USA), taking care that the cut surface was fully immersed. The sodium hexametaphosphate solution represents a C-free polyphosphate buffer binding calcium ions and therefore reducing callose blocking of sieve tubes (Gessler *et al.*, 2004). In pre-experiments, it was found that exudation was high during the first hour before reaching a lower, but constant rate. This initial maximum was likely to have been caused by leakage from wounded parenchyma cells during the first hour. Therefore, exudates from the first hour were discarded and the vials replaced by new ones, containing the same amount of solution. Collection of exudate was stopped after 5 h and the leaf area determined. Phloem samples from individual leaves were pooled for each plant and time point. To remove polyphosphate buffer and ionic components, samples were ion-exchanged as described above. Concentration and isotopic composition of the phloem sugars were determined with HPLC-IRMS (see below).

Compound-specific isotope analysis of sugars and organic acids

For compound-specific isotope analysis, an HPLC system (Dionex Corporation, Sunnyvale, CA, USA) was coupled to a Finnigan Delta V Advantage Mass Spectrometer by a Finnigan LC IsoLink Interface (Thermo Fisher Scientific, Waltham, MA, USA). In the first step, sample compounds were separated by the HPLC system, consisting of an ICS-3000 pump (directly supplied with deionized water by an ICW-2000 device, Millipore Corporation, Billerica, MA, USA), an AS50 autosampler with a 25 µl sample loop and an Ultimate 3000 column compartment (Dionex Corporation). Columns and eluents used for the separation of sugars and organic acids are described below. In the second step, the separated compounds were oxidized to CO_2 in the Finnigan LC IsoLink Interface (Krummen *et al.*, 2004). As oxidant and acid reagents, 0.5 M sodium persulphate (sodium peroxodisulphate purum p.a., ≥99%, Fluka, Sigma-Aldrich) and 1.7 M phosphoric acid (ortho-phosphoric acid puriss. p.a., crystallized, ≥99%, Fluka, Sigma-Aldrich), respectively, were used. Flow rates of both reagents were 50 µl min^{-1}, and oxidation temperature was 99.9 °C. In the third step, excess O_2 was removed as described by Hettman *et al.* (2007): Two ceramic tubes (length 30 cm, diameter 1 mm, Friatec AG, Mannheim, Germany) were filled with copper wire (30 wires each, diameter 50 µm, Goodfellow Cambridge Ltd., Huntington, UK), and heated to 580 °C in a furnace (MTF 10/15/130 with a Carbolite 301 temperature controller, Carbolite Ltd., London, UK). A two-position eight-port valve (EC8WE, VICI AG International, Schenkon, Switzerland) switched between the sample stream (He) and H_2 (1% H_2 in He), with one of the tubes being oxidized by the O_2 in the sample stream and one reduced at a time. Finally, the O_2-free gas stream was transferred to the mass spectrometer for stable isotope analysis.

For sugar separation, a HyperREZ XP Carbohydrate Pb^{2+} 8 µm column (Thermo Fisher Scientific) was used at 80 °C and with 0.6 ml min^{-1} of deionized water as eluent, which allowed baseline separation of sucrose, fructose, and an unidentified component X1 in the tissue saps. Glucose could not be fully separated from another unidentified component X2, potentially affecting glucose C isotope values. Samples were measured and compared with standard solutions to calculate the concentrations and correct for $\delta^{13}C$ offset. Standards were referenced with EA/IRMS (EA 1110, CE Instruments, Milan, Italy, coupled to a Finnigan MAT Delta Plus IRMS, Thermo Fisher Scientific) as pure chemicals (n=3) before preparing the solutions. As standards, two stock solutions of sucrose, glucose, and fructose with $\delta^{13}C$ values ranging from –27‰ to –10‰ were prepared, diluted to different concentrations (12.5–300 mg l^{-1}), and analysed interspersed with the samples. Peak areas and concentrations of standards showed a linear correlation which was used to calculate the concentrations of the samples. Measurement of $\delta^{13}C$ with HPLC-IRMS showed an offset from EA/IRMS, depending on sample concentration. To correct for the offset, a multiple regression equation of the following form was applied:

$$\delta_{offline} = a \times \text{peak area} + b \times \delta_{online} + c$$

where $\delta_{offline}$ and δ_{online} represent the $\delta^{13}C$ values of the standards measured by EA/IRMS and HPLC-IRMS, respectively. $\delta^{13}C$ values of each sample compound were corrected by inserting a, b, c (calculated from the respective standards), peak area, and δ_{online} (from HPLC-IRMS analysis of the sample) into the equation. Average standard deviations of $\delta^{13}C$ values were 0.06‰ for sucrose, 0.10‰ for glucose, and 0.13‰ for fructose (n=3, for standards ranging from 25–200 mg l^{-1}).

For organic acids, an ion pack AS11 4 mm column (Dionex Corporation) was selected, at a flow rate of 0.35 ml min^{-1} and 25 °C. As eluent, a KOH gradient from 2–25 mM was used. KOH was generated online by an EGC II KOH eluent generator cartridge, controlled by an RFC-30 device (Dionex Corporation), and removed after HPLC separation by an ASRS Ultra 2 mm suppressor (Dionex Corporation). As well as malate, samples contained high amounts of citrate and isocitrate, which could not be completely separated and are therefore represented as combined citrate/isocitrate values. As standards, a concentration series of malate and isocitrate (12.5–300 mg l^{-1}) was analysed with the samples. Calculation of sample concentrations and correction for $\delta^{13}C$ offset were performed as for sugars. Average standard deviations of $\delta^{13}C$ values were 0.06‰ for malate, 0.08‰ for citrate, and 0.09‰ for isocitrate (n=3, for standards ranging from 12.5–300 mg l^{-1}).

Determination of isotopic composition and concentration of starch

The determination of isotopic composition and amount of starch in leaves was based on an enzymatic digestion as previously described (Gottlicher *et al.*, 2006; Richter *et al.*, 2009) with the slight modification that only 50 mg of plant material was used.

Gas exchange and instantaneous discrimination

For the determination of net CO_2 exchange, whole plant shoots were sealed into custom-built plexiglass chambers equipped with ventilators, the root system being outside the chambers. Dried ambient air (pCO_2=409.4±2.5 ppm, n=113, and $\delta^{13}C$= –10.0±0.2‰, n=27, mean ±SE) was directed through the chambers and analysed by an infrared gas analyser (ADC 225-MK3, ADC Bioscientific Ltd., Herts, UK). A WA-161 device (ADC Bioscientific Ltd.) switched between air from the two chambers and the unaltered reference gas stream (ambient air). Flow rates were determined with

mass flow meters installed in front of the chambers and leaf temperature was measured with thermo elements. After the end of the experiment, plants were harvested and leaves scanned to determine the leaf area. Net photosynthesis (*NP*; in μmol m^{-2} s^{-1}) was calculated as

$$NP = \frac{(c_r - c_s) \times V_{20}}{MolVol_{20} \times a \times 60}$$

where V_{20} (l min^{-1}) is the flow of gas through the chamber corrected for the deviation from standard conditions of 20 °C and 1000 mBar air pressure as

$$V_{20} = \frac{f \times 293.15 \times p}{(273.15 + T) \times 1000}$$

c_r and c_s represent the CO_2 partial pressure of reference and sample gas (ppm), respectively, a is the leaf area (m^2), $MolVol_{20}$ denotes the volume of 1 mol gas under standard conditions, f is the flow of gas through the chamber measured by the mass flow meter (l min^{-1}), T is the ambient temperature (°C), and p is the air pressure (mBar) inside the chamber. Transpiration was not measured.

For the determination of instantaneous discrimination ($\Delta^{13}C$), gas samples were taken by connecting a syringe to the IRGA outlet. The samples were immediately transferred into pre-evacuated gas containers (IVA 738W, IVA Analysentechnik, Meerbusch, Germany), stored at 4 °C and analysed within 7 d. $\delta^{13}C$ of CO_2 was measured on a Finnigan GasBench coupled to a Finnigan Delta V Advantage Mass Spectrometer (Thermo Fisher Scientific). $\Delta^{13}C$ (‰) was calculated according to Evans *et al.* (1986), as

$$\Delta = \frac{\xi(\delta_s - \delta_r)}{1000 + \delta_s - \xi(\delta_s - \delta_r)} \times 1000$$

where $\xi = c_r/(c_r - c_s)$, and δ_r and δ_s are $\delta^{13}C$ values of the reference and sample gas, respectively. Each data point represents the average of three consecutive measurements for a single plant.

Carbon budgets

Fixation of external CO_2 (M_{ext}) was calculated from the gas exchange measurements. Subtraction of $\Delta^{13}C$ from $\delta^{13}C$ of reference gas of the respective phase gave $\delta^{13}C$ of CO_2 taken up. The amount (M_{resp}) and $\delta^{13}C$ (δ_{resp}) of respiratory CO_2 refixed in phase I were calculated based on Borland (1996) from malate accumulation (M_m and δ_m), uptake of external CO_2 (M_{ext} and δ_{ext}), and the amount of degraded starch necessary for C skeletons ($M_m \times 3/4$ and δ_{st}), assuming one C per malate coming from CO_2 (either external or respiratory) and three from starch degradation, as

$$M_{resp} = \frac{M_m}{4} - M_{ext}$$

and

$$\delta_{resp} = \frac{\delta_m \times M_m - \delta_{st} \times M_m \times \frac{3}{4} - \delta_{ext} \times M_{ext}}{M_{resp}}$$

To estimate the proportions of PEPC and direct Rubisco fixation during phase II, a mass balance equation was applied, setting PEPC $\Delta^{13}C$ to the night-time value and Rubisco $\Delta^{13}C$ to the maximum reached at the end of phase II when pure C_3 fixation was likely:

$$\delta_{C3} \times M_{C3} + \delta_{C4} \times M_{C4} = \delta_{II} \times M_{II}$$

and

$$M_{C3} + M_{C4} = M_{II}$$

M_{C3}, δ_{C3}, M_{C4}, and δ_{C4} represent amounts and $\delta^{13}C$ values of C fixed by Rubisco and PEPC (calculated by subtraction of $\Delta^{13}C$ from $\delta^{13}C$ of phase II reference gas), respectively, and M_{II} and δ_{II} of total C fixed during phase II.

For the analysis of cellular C partitioning, malate, starch, and sucrose were considered, which exhibited the largest changes in concentration (malate, starch) or isotopic composition (sucrose) and are thus supposed to have the highest turnover. If $\delta^{13}C$ values changed significantly over a certain phase ($P < 0.1$), the isotopic composition of the net flux was calculated with mass balance equations (Deleens and Garnier-Dardart, 1977).

Starch was assumed to provide the C skeletons for malate synthesis in phase I (with three carbons from starch per carbon fixed). A scheme of the C fluxes that were considered (modified after Dodd *et al.*, 2002) is presented in Fig. 1. The contribution of C fixed by PEPC and directly by Rubisco to phloem sucrose was calculated with a mixing model using the average $\delta^{13}C$ values of C fixed by the respective enzyme, and the weighted average of phloem sucrose $\delta^{13}C$ values. No isotopic discrimination during leaf export was assumed. $\delta^{13}C$ values of phloem sucrose were compared with those of leaf sucrose at different time points (measured values plus several integrated values) to analyse the strength of correlation and, eventually, the time-lag for phloem exudation.

Statistical analysis

Statistical analysis was performed with Statistica 6.0 (StatSoft, Inc., Tulsa, OK, USA). Normal distribution of the data was checked with the Lilliefors test (95%). One-way ANOVA with the Tukey HSD test was applied to calculate levels of significance.

Results

Gas exchange and instantaneous discrimination

A typical four-phase gas exchange pattern was observed (Fig. 2). The major proportion of CO_2 was fixed during phase I by PEPC. During this time, respiratory refixation accounted for 27% of total fixation (Table 1). With the onset of light and the start of phase II, CO_2 uptake increased sharply, concurrent with an increase in the instantaneous discrimination from 1‰ to 15‰ due to a shift from PEPC to

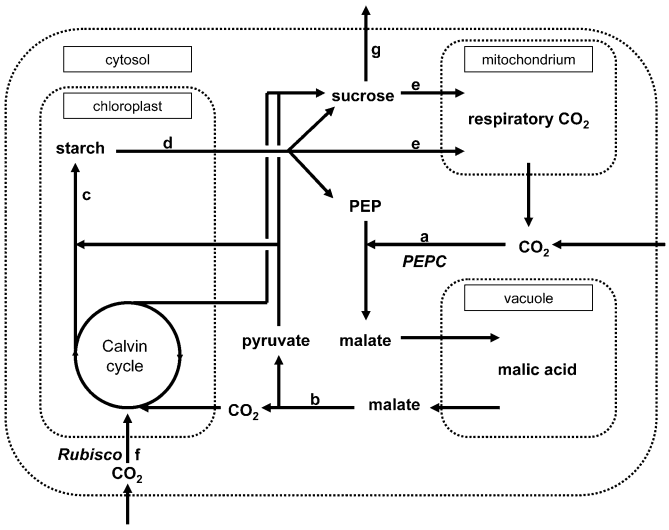

Fig. 1. Proposed scheme of cellular carbon flow in *K. daigremontiana*, modified after Dodd *et al.* (2002), focusing on the sucrose pool. PEPC fixation, a; malate decarboxylation, b; starch accumulation, c; starch degradation, d; respiration, e; Rubisco fixation, f; export, g.

Rubisco fixation. After about 3 h of light, stomata closed, marking the onset of phase III. During this time, only minimal net gas exchange was observed. CO_2 uptake increased in the late afternoon (phase IV), with instantaneous discrimination reaching 17‰ at the end of the phase, indicating a high proportion of direct Rubisco fixation. The lower discrimination in the beginning may have been due to stomatal limitation rather than to a temporary activation of PEPC. Altogether, PEPC fixation accounted for 85% of overall C fixation, while direct Rubisco fixation accounted for 15%.

Concentration and isotopic composition of starch and organic acids

Concentrations of malate and starch changed significantly over the diurnal cycle (P <0.00001 and P <0.000001, respectively), whereas no significant differences could be observed for citrate/isocitrate (Fig. 3). As expected, degradation of starch and accumulation of malate occurred in phase I, and vice versa in phase III. In phases II and IV, no significant net change of malate or starch levels was observed (Table 2), although instantaneous discrimination during phase II indicated a high rate of PEPC fixation, suggesting decarboxylation of phase II malate immediately after its synthesis.

Malate $\delta^{13}C$ values were close to the value of CO_2 fixed by PEPC and only slightly varied over the course of the day (range 1.4‰, P=0.0003). Starch was depleted in ^{13}C compared to malate by about 1.5‰ and showed only non-significant changes over the diurnal cycle that can be explained by a large, isotopically inhomogenous starch background.

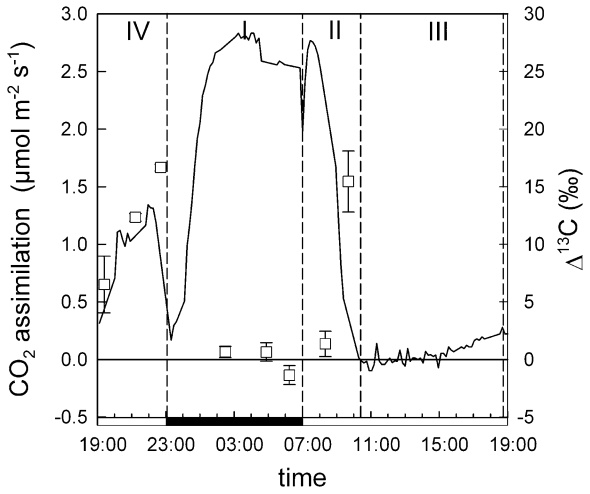

Fig. 2. Diurnal pattern of net CO_2 uptake (solid line) and instantaneous discrimination $\Delta^{13}C$ (squares) of an exemplary *K. daigremontiana* plant. CAM phases are denoted by dashed lines, the solid bar on the *x*-axis indicates the dark period. $\Delta^{13}C$ is shown as the mean ±SE of three consecutive measurements.

Table 1. CO_2 fixation (mean, n=2), instantaneous discrimination ($\Delta^{13}C$; mean, n=3) and $\delta^{13}C$ of fixed CO_2

Phase	Time	CO_2 fixation (mg C g^{-1} DW)	$\Delta^{13}C$ (‰)	$\delta^{13}C$ (‰)
Phase I	23:20–07:00 h	8.92		–11.28
External fixation		6.54	–0.01	–10.22
Respiratory refixation		2.38		–14.22
Phase II	07:00–10:20 h	1.88		–11.88
Direct Rubisco fixation		0.34	15.45	–24.62
PEPC fixation		1.55	(–0.01)	–9.09
Phase III	10:20–18:40 h	0.14		
Phase IV	18:40–23:20 h	1.41	11.84	–22.38
Total external fixation		9.98	2.11	–12.28
Total fixation		12.36		–12.66
Total direct Rubisco fixation		1.89		–22.81
Total PEPC fixation		10.46		–10.96

Concentration and isotopic composition of soluble sugars

Compound-specific stable isotope analysis with HPLC-IRMS revealed remarkable differences between diurnal patterns of soluble sugars in both concentration and isotopic composition. Glucose and fructose concentrations were highly correlated, both exhibiting non-significant decreases during the night and increases during the day.

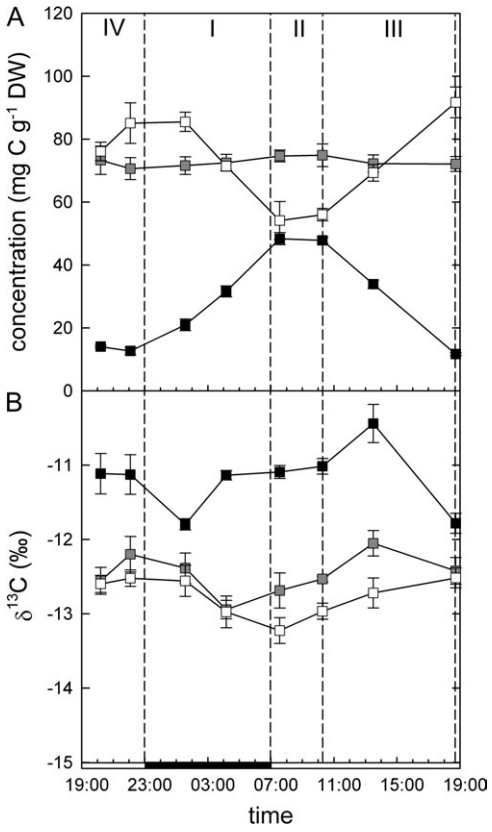

Fig. 3. Diurnal changes in the concentration (A) and $\delta^{13}C$ (B) of starch (open symbols), malate (closed symbols), and citrate/isocitrate (shaded symbols) of *K. daigremontiana*. CAM phases are denoted by dashed lines, the solid bar on the *x*-axis indicates the dark period. Data shown are the means ±SE of five replicate plants.

Table 2. Change of size and isotopic composition of pools between start and end of each phase (*P* values were calculated by ANOVA, followed by Tukey HSD test)

Net flux $\delta^{13}C$ values were calculated by applying mass balance equations, if changes were marginally significant (P <0.1). Pool $\delta^{13}C$ values are averages of the respective phase.

Phase	Pool	Net flux size		Net flux $\delta^{13}C$		Pool $\delta^{13}C$
		(mg C g^{-1} DW)	*P* value	(‰)	*P* value	(‰)
I	Malate	35.67	0.0001		1.0000	–11.29
I	Starch	–30.98	0.0003	–11.29	0.0789	–12.82
I	Sucrose	0.54	0.1083	0.59	0.0001	–14.37
II	Malate	–0.52	1.0000		0.9994	–11.02
II	Starch	1.88	1.0000		0.9467	–13.10
II	Sucrose	0.82	0.0027	–16.94	0.0027	–12.62
III	Malate	–36.15	0.0001	–10.69	0.0493	–11.06
III	Starch	35.68	0.0001		0.5412	–12.73
III	Sucrose	–1.32	0.0001		0.9978	–13.45
IV	Malate	1.00	0.9995		0.2006	–11.34
IV	Starch	–6.58	0.9421		1.0000	–12.55
IV	Sucrose	–0.05	1.0000	97.37	0.0001	–15.10

Sucrose, on the other hand, showed strong and highly significant changes in concentration (P <0.000001). Sucrose concentration started to increase in the morning and reached a maximum at the end of phase II, then decreased to the initial value at the end of phase III (Fig. 4).

$\delta^{13}C$ values of glucose and fructose remained constant over the diurnal cycle. By contrast, mean sucrose $\delta^{13}C$ values ranged between –17‰ and –12‰ (P <0.000001). The lowest $\delta^{13}C$ values of sucrose were observed at the end of phase IV, representing the highest contribution of C derived from Rubisco fixation to the sucrose pool (Fig. 4). During phase I, $\delta^{13}C$ of sucrose increased, reaching the maximum at the end of the phase, then slightly declined during phase II and remained constant until phase IV, when it started to decline again.

Sucrose accounted for about 70% of phloem sugars and was the only sugar with concentrations sufficient for $\delta^{13}C$ analysis. $\delta^{13}C$ values of phloem sucrose exhibited significant differences over the diurnal cycle (P <0.000001; Fig. 5). The lowest values were observed in phase I, several hours after the leaf sucrose pool had reached its lowest value. $\delta^{13}C$ values of phloem and leaf sucrose (δ_p and δ_l, respectively) showed the best correlation when a time-lag of 5 h was assumed (r^2=0.9973, P=0.0013; $\delta_p = 0.97 \times \delta_l - 1.30$).

Carbon budgets

The gas exchange data (Table 1) and changes in pool size and isotopic composition of malate, starch, and sucrose (Table 2) were combined to model leaf C flows (as outlined in Fig. 1). Malate and starch net fluxes were much higher than sugar and CO_2 net fluxes (Table 2). In phase I, 86% of C from starch degradation was necessary to provide the cell with C for malate synthesis (assuming that three-quarters of the C accumulated as malate came from starch

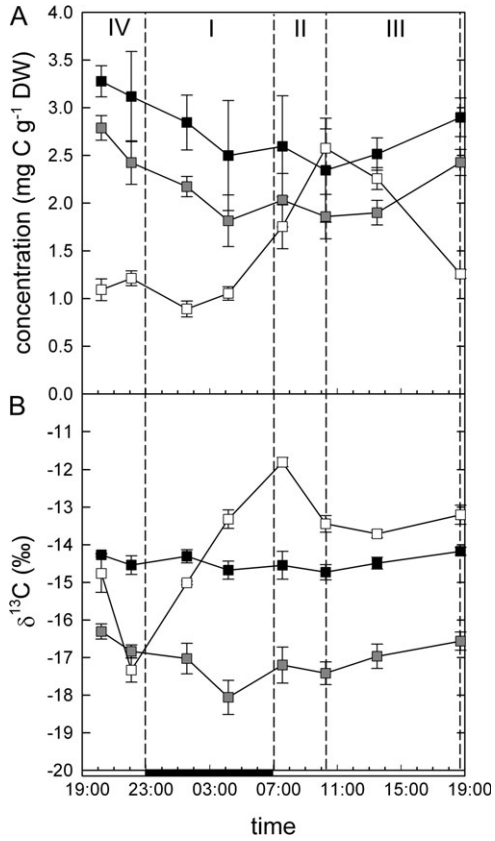

Fig. 4. Diurnal changes in the concentration (A) and $\delta^{13}C$ (B) of sucrose (open symbols), fructose (closed symbols), and glucose (shaded symbols) of *K. daigremontiana*. CAM phases are denoted by dashed lines, the solid bar on the *x*-axis indicates the dark period. Data shown are the means ±SE of five replicate plants. At the end of the phases I, II, III, and IV, carbon from direct Rubisco fixation accounted for 7, 21, 19, and 54% of sucrose, respectively.

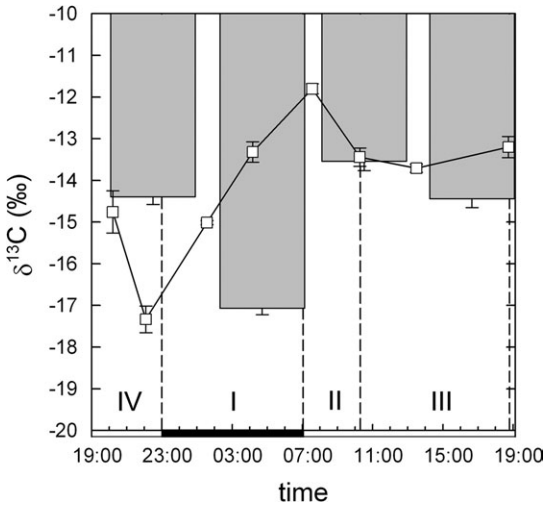

Fig. 5. Diurnal changes in $\delta^{13}C$ of sucrose in the leaf (squares) and in phloem exudates (shaded bars) in *K. daigremontiana*. Exudation lasted 5 h. The phases are denoted by dashed lines, the solid bar on the *x*-axis indicates the dark period. Data shown are the means ±SE of five replicate plants.

degradation), and 10% for dark respiration (calculated from respiratory re-fixation; Table 1). The calculated $\delta^{13}C$ value of dark respiration suggests that the C had passed through the sucrose pool before being respired (–14.22 versus –14.37‰; Tables 1, 2). In phase III, 99% of C from malate decarboxylation (including both released CO_2 and pyruvate) were accumulated as starch. In phases II and IV, only minor net fluxes of malate and starch were observed.

Discussion

Based on their turnover rates, three types of metabolic C pools could be distinguished. First, malate and starch showed a diurnal pattern of reciprocal mobilization and accumulation (Fig. 3), with 99% of C from phase III malate decarboxylation used for starch accumulation and 86% of C from phase I starch degradation used to provide C skeletons. Average $\delta^{13}C$ values of –11‰ and –13‰ (for malate and starch, respectively) demonstrated the pivotal contribution of PEPC fixation (average $\delta^{13}C$ of PEPC fixation –11‰) to these pools. Second, glucose and fructose exhibited low turnover rates. Both concentration and isotopic composition remained constant over the diurnal cycle. Third, sucrose showed rapid and highly significant (P <0.000001) changes of $\delta^{13}C$ values, ranging between –17‰ and –12‰ (Fig. 4). The strongest isotopic changes in sucrose occurred during phases I and IV, when concentrations were nearly constant (Table 2). If only influx into the sucrose pool was responsible for the ^{13}C enrichment during phase I, C entering must have had a $\delta^{13}C$ of 0.59‰ (Table 2); which is extremely unlikely. Therefore, a high flow through the sucrose pool has to be assumed where ^{13}C-enriched C enters and comparatively ^{13}C-depleted C leaves the pool, as supported by the depleted values of phloem sucrose in phase I (Fig. 5). The same can be concluded for phase IV, where a small efflux of sucrose with 97.37‰ would be necessary to explain the changes of isotopic composition, if no import into the pool was assumed. Both results point to a high turnover of the sucrose pool during the diurnal cycle.

Furthermore, from the changes in leaf sucrose $\delta^{13}C$ values, it is obvious that C influx in phases II and IV predominantly originated from direct Rubisco fixation, which was also supported by the increase in sucrose concentration during phase II. During phase I, however, the C influx was coming from a PEPC-derived pool—presumably starch. Carbon flux from malate decarboxylation to sucrose in phase III must have been minimal, as sucrose $\delta^{13}C$ values did not reach the comparatively enriched malate values. Comparing the $\delta^{13}C$ values of dark respiration (–14.22‰), C derived from phase I starch degradation (–11.29‰), and the phase I sucrose pool (–14.37‰), one may speculate that the sucrose pool was the main substrate for dark respiration. It is therefore likely that the nocturnal starch degradation was not only a source of PEP for PEPC fixation, but was also fuelling the leaf sucrose pool, which, in turn, was the source of dark respiration and phloem export.

The demonstration of three pool types—CAM maintenance carbon, low turnover hexoses, and high turnover sucrose—in this study supports previous postulations of C partitioning within plant leaves: For *Kalanchoë* spp., two distinct glycolytic pathways during phase I were suggested by Deleens and Garnier-Dardart (1977) and Deleens *et al.* (1979), with starch as the source of C skeletons on the one hand and soluble sugars as the substrate for dark respiration on the other hand. A similar compartmentation was demonstrated for *Sedum telephium* L. (Borland and Griffiths, 1996). Two distinct sugar pools were suggested for *Clusia* spp., which uses soluble sugars instead of starch for CAM maintenance: A vacuolar sugar pool from PEPC fixation, used as a substrate for malate synthesis, as opposed to a high turnover cytosolic sugar pool from direct Rubisco fixation, fuelling phloem export (Borland and Dodd, 2002; Borland *et al.*, 1994).

In this study, direct Rubisco fixation accounted for 30% of phloem sucrose C, but only for 15% of total CO_2 fixation. Thus, a preference of C fixed directly by Rubisco from atmospheric CO_2 during phases II and IV for export was demonstrated. It is unlikely that the time lag of 5 h between leaf and phloem sucrose $\delta^{13}C$ values was caused by the distance for transport (about 2 cm), but rather by differences between cellular sucrose pools (e.g. vacuolar versus cytosolic pool), which are likely considering the high turnover of the total sucrose pool that was found (Fig. 4).

As both Rubisco and PEPC-derived C are contributing to the leaf sucrose pool, a shift in the relationship between PEPC and direct Rubisco fixation will strongly affect the isotopic composition of the leaf sucrose pool and, in consequence, of phloem sap and sink tissues. This relationship may depend on plant species, developmental stage and especially on environmental parameters: For *K. daigremontiana*, Griffiths *et al.* (2002) demonstrated that a reduced water supply resulted in an increase in nocturnal CO_2 uptake, whereas phases II and IV almost disappeared. Temperature was also shown to affect CO_2 exchange of *K. daigremontiana* with phase II fixation being reduced when temperature increased (Winter and Tenhunen, 1982). A higher proportion of direct Rubisco fixation might, therefore, result in a clear Rubisco signal of exported C, in spite of PEPC fixation.

By taking up CO_2 at night, CAM plants manage to deal with low or intermittent water supply, but the associated elevated energy demand and the necessity of large carbohydrate stocks for CAM maintenance are limiting productivity. Thus, curtailing the competition between C storage for CAM maintenance and export for growth is of crucial importance for this type of plant. CAM plants have to store as much C as necessary to maintain a high capacity to fix CO_2, but yet to export as much as possible for growth. Furthermore, as both the available amount of C and the nocturnal demand for C skeletons are influenced by environmental conditions, control mechanisms have to be highly adaptive. By using PEPC-fixed C preferentially for refilling leaf carbohydrate stocks, the amount of C stored

for CAM maintenance is directly controlled by the amount of C fixed by CAM in the previous night—and thus by the expected C demand in the following night. While 99% of C from phase III malate decarboxylation was accumulated as starch in this study, only 86% of C from nocturnal starch degradation was required for malate synthesis. The remaining 14% of starch-derived C, as well as C from direct Rubisco fixation, were available for other purposes such as phloem export.

In summary, it was possible to demonstrate by direct measurements that carbon fixed in different CAM phases is not equally used for growth or maintenance. Carbon fixed directly by Rubisco during phases II and IV was preferentially, but not exclusively, utilized for export to the stem and roots.

Acknowledgements

Stable isotope analysis was performed in the SILVER facility (Stable Isotope Laboratory at the University of Vienna for Environmental Research). We thank Margarete Watzka for EA/IRMS and GasBench analysis, and Andreas Blöchl for assistance with the HPLC system.

References

Borland AM. 1996. A model for the partitioning of photosynthetically fixed carbon during the C3-CAM transition in *Sedum telephium*. *New Phytologist* **134,** 433–444.

Borland AM, Dodd AN. 2002. Carbohydrate partitioning in Crassulacean acid metabolism plants: reconciling potential conflicts of interest. *Functional Plant Biology* **29,** 707–716.

Borland AM, Griffiths H. 1996. Variations in the phases of Crassulacean acid metabolism and regulation of carboxylation patterns determined by carbon-isotope-discrimination techniques. *Ecological Studies* **114,** 230–249.

Borland AM, Griffiths H, Broadmeadow MSJ, Fordham MC, Maxwell C. 1994. Carbon-isotope composition of biochemical fractions and the regulation of carbon balance in leaves of the C_3-Crassulacean acid metabolism intermediate *Clusia minor* L growing in Trinidad. *Plant Physiology* **106,** 493–501.

Christopher JT, Holtum JAM. 1996. Patterns of carbon partitioning in leaves of Crassulacean acid metabolism species during deacidification. *Plant Physiology* **112,** 393–399.

Deleens E, Garnier-Dardart J. 1977. Carbon isotope composition of biochemical fractions isolated from leaves of *Bryophyllum daigremontianum* Berger, a plant with Crassulacean acid metabolism: some physiological aspects related to CO_2dark fixation. *Planta* **135,** 241–248.

Deleens E, Garnier-Dardart J, Queiroz O. 1979. Carbon isotope composition of intermediates of the starch-malate sequence and level of the Crassulacean acid metabolism in leaves of *Kalanchoë blossfeldiana* Tom Thumb. *Planta* **146,** 441–449.

Dodd AN, Borland AM, Haslam RP, Griffiths H, Maxwell K. 2002. Crassulacean acid metabolism: plastic, fantastic. *Journal of Experimental Botany* **53,** 569–580.

Dodd AN, Griffiths H, Taybi T, Cushman JC, Borland AM. 2003. Integrating diel starch metabolism with the circadian and environmental regulation of Crassulacean acid metabolism in *Mesembryanthemum crystallinum*. *Planta* **216,** 789–797.

Evans JR, Sharkey TD, Berry JA, Farquhar GD. 1986. Carbon isotope discrimination measured concurrently with gas-exchange to investigate CO_2diffusion in leaves of higher plants. *Australian Journal of Plant Physiology* **13,** 281–292.

Farquhar GD, Ehleringer JR, Hubick KT. 1989. Carbon isotope discrimination and photosynthesis. *Annual Review of Plant Physiology and Plant Molecular Biology* **40,** 503–537.

Gessler A, Rennenberg H, Keitel C. 2004. Stable isotope composition of organic compounds transported in the phloem of European beech: evaluation of different methods of phloem sap collection and assessment of gradients in carbon isotope composition during leaf-to-stem transport. *Plant Biology* **6,** 721–729.

Gottlicher S, Knohl A, Wanek W, Buchmann N, Richter A. 2006. Short-term changes in carbon isotope composition of soluble carbohydrates and starch: from canopy leaves to the root system. *Rapid Communications In Mass Spectrometry* **20,** 653–660.

Griffiths H, Broadmeadow MSJ, Borland AM, Hetherington CS. 1990. Short-term changes in carbon-isotope discrimination identify transitions between $C_3$and C_4carboxylation during Crassulacean acid metabolism. *Planta* **181,** 604–610.

Griffiths H, Cousins AB, Badger MR, von Caemmerer S. 2007. Discrimination in the dark. Resolving the interplay between metabolic and physical constraints to phosphoenolpyruvate carboxylase activity during the Crassulacean acid metabolism cycle. *Plant Physiology* **143,** 1055–1067.

Griffiths H, Helliker B, Roberts A, Haslam RP, Girnus J, Robe WE, Borland AM, Maxwell K. 2002. Regulation of Rubisco activity in Crassulacean acid metabolism plants: better late than never. *Functional Plant Biology* **29,** 689–696.

Hettmann E, Brand WA, Gleixner G. 2007. Improved isotope ratio measurement performance in liquid chromatography/isotope ratio mass spectrometry by removing excess oxygen. *Rapid Communications In Mass Spectrometry* **21,** 4135–4141.

Krummen M, Hilkert AW, Juchelka D, Duhr A, Schluter HJ, Pesch R. 2004. A new concept for isotope ratio monitoring liquid chromatography/mass spectrometry. *Rapid Communications In Mass Spectrometry* **18,** 2260–2266.

Mayoral ML, Medina E. 1985. ^{14}C-translocation in *Kalanchoë pinnata* at two different stages of development. *Journal of Experimental Botany* **36,** 1405–1413.

Nobel PS. 1991. Achievable productivities of certain CAM plants: basis for high values compared with C_3 and C_4 plants. *New Phytologist* **119,** 183–205.

Osmond CB. 1978. Crassulacean acid metabolism: curiosity in context. *Annual Review of Plant Physiology and Plant Molecular Biology* **29,** 379–414.

Popp M, Lied W, Meyer AJ, Richter A, Schiller P, Schwitte H. 1996. Sample preservation for determination of organic compounds: microwave versus freeze-drying. *Journal of Experimental Botany* **47,** 1469–1473.

Richter A, Wanek W, Werner RA, *et al*. 2009. Preparation of starch and soluble sugars of plant material for the analysis of carbon isotope composition: a comparison of methods. *Rapid Communications In Mass Spectrometry* **23,** 2476–2488.

Winter K, Holtum JAM. 2002. How closely do the $\delta^{13}C$ values of Crassulacean acid metabolism plants reflect the proportion of CO_2fixed during day and night? *Plant Physiology* **129,** 1843–1851.

Winter K, Smith JAC. 1996. An introduction to Crassulacean acid metabolism. Biochemical principles and ecological diversity. In: Winter K, Smith JAC, eds. *Crassulacean Acid Metabolism: Biochemistry, Ecophysiology and Evolution*. Berlin: Springer, 1–13.

Winter K, Tenhunen JD. 1982. Light-stimulated burst of carbon-dioxide uptake following nocturnal acidification in the Crassulacean acid metabolism plant. *Kalanchoë daigremontiana. Plant Physiology* **70,** 1718–1722.